Optical emission from electrons in solid deuterium tritium

F. Magnotta, G. W. Collins, and E. R. Mapoles
Lawrence Livermore National Laboratory, Livermore, California 94551
(Received 10 January 1994)

We report an increase in an emission from solid deuterium tritium at 825 nm, while pumping an electron bubble transition centered at ~350 nm. This experiment implies unbound electrons cause the emission at 825 nm. We find this steady-state emission shifts 8 nm towards longer wavelengths upon increasing the temperature from 4.5 to 10 K. Finally, the same emission in pure solid T_2 is shifted 3 nm towards longer wavelengths and contains a triplet structure similar to the triplet structure observed in absorption measurements of the $1S$ to $1P$ transition of electron bubbles.

I. INTRODUCTION

The discovery of trapped ions in tritiated solid hydrogen was made by Souers *et al.* through the observation of Stark shifted lines in the collision-induced infrared (IR) absorption spectra of solid hydrogen.[1] Two new IR absorption lines were found at 100 and 25 cm^{-1} below $Q_1(1,0)$. Positive ions contract neighboring molecules giving rise to larger Stark shifts than negative ions which push neighboring molecules away due to the Fermi interaction. Thus, the absorptions 100 and 25 cm^{-1} below $Q_1(1,0)$ are assigned to Stark shifted $Q_1(1,0)$ transitions for molecules near positive and negative ions, respectively. There have also been weak absorptions found in between these two Stark shifted transitions that have been assigned to next-nearest neighbors of the positive ion.[2] From on-off timing experiments in proton irradiated solid D_2, Brooks *et al.* determined that there were at least two types of positive charges and negative charges. The most mobile was identified as a negatively charged polaron, then a D_3^+ "small polaron hole," while a D_9^+ and "trapped" electrons or electron bubbles were determined to be immobile over the period of hours.[3]

After the discovery of these Stark shifted lines, two broad absorptions, not related to the collision-induced hydrogen spectra, were observed in tritiated solid hydrogen and in proton-irradiated solid hydrogen.[4-7] These transitions are located at ~350 nm and ~1.5 μm in solid deuterium tritium. In analogy with F centers in alkali halides and electron bubbles in liquid helium, it was postulated that these two absorptions were due to transitions between electron bubble states. From a simple spherical square-well model, the electron bubble radius was determined to be 0.54 nm with a well depth of 3.8 eV.[5] It was estimated by Poll *et al.*[5] that an electron in the first excited state would dilate the lattice an additional 15%. The IR absorption band was assigned to the $1S$ to $1P$ transition and the UV absorption was assigned to the $1S$ to continuum transition. There appeared to be an isotope shift in both the IR and UV transitions, and the UV band was broader in H_2 than in D_2 both doped with tritium, implying a broader conduction band in H_2 than D_2. This result is similar to the work of Gedanken, Raz, and Jortner[8] who studied trapped excitations in solid H_2 and D_2.

We then reported a broadband emission at 825 nm (Ref. 9) in solid D-T (a mixture of 25% D_2, 50% DT, 25% T_2) at 6.4 K. The intensity of this emission has a temperature dependence similar to that of the hydrogen atoms in D-T as measured by electron-spin resonance (ESR). This does not yield a precise cause for the emission since at temperatures between half the triple point and the triple point, diffusion of molecules in H_2 and D_2,[10] atomic hydrogen in H_2 and D_2,[11,12] and excess electrons in para-H_2,[13] all follow the same vacancy diffusion model of Ebner and Sung.[14] The emission at 825 nm was later observed by groups at the University of Guelph and the EURATOM-Risø National Laboratory[15] using proton-beam and electron-beam irradiation of solid D_2, respectively. No assignment has been given to this emission, and correlation with previous absorption features seemed dubious since the timing data for this emission was very different than the timing data for the Stark shifted collision-induced lines and the IR and UV lines. In this paper we will refer to this emission feature as the "825-nm" emission even though that specific line position occurs in D-T only at 6.4 K.

To summarize, all of the spectral features discussed above are due to immobile species which go away above ~10 K. These species have been assumed to be D_9^+ and electron bubbles. No spectral features are attributed to mobile carriers, assumed to be D_3^+ and small polarons.

We report here a relatively large increase in emission of the integrated 825-nm line in solid D-T when pumping the UV absorption and a smaller increase (by a factor of ~2) upon pumping near the IR absorption. These data show the 825-nm emission is related to unbound electrons in irradiated solid hydrogen. The steady-state 825-nm emission, shifts 8 nm towards longer wavelengths upon increasing the temperature from 4.5 to 10 K. Finally, the same emission in pure solid T_2, is shifted ~3 nm towards longer wavelengths and contains a triplet structure similar to the triplet structure observed in absorption measurements of the $1S$ to $1P$ transition of electron bubbles. These experiments imply the emission is related to the electron bubble.

II. EXPERIMENTAL PROCEDURE

The experimental paradigm for collecting the enhanced emission data is to shine both pulsed and cw light onto a tritiated deuterium sample at 4.5 K, vary the wavelength and observe the response of the steady-state 825-nm emission feature. The sample cell was a 0.8-mm-diameter spherical glass shell with a 2-μm-thick wall. The shell was filled with D-T gas by permeation to $\sim$25 atm and then attached to a copper standoff wire centered at the focus of a gold-plated parabolic mirror. The mirror and sample holder assembly were in turn attached to the cold tip of a helium flow cryostat capable of varying and controlling the sample temperature from 4.5 to 30 K. Optical access to the sample was through two MgF_2 windows at normal incidence. Experiments were performed using both laser and lamp sources. Steady-state experiments were performed from 345 to 700 nm using a 150 Watt xenon lamp and from 1.15 to 2.00 μm using a tungsten halogen lamp. In the UV and visible regions, the xenon lamp was dispersed by a monochrometer fitted with various long pass, order sorting filters, to block unwanted higher frequency radiation. The bandpass was set at 10 nm and the incident power set to approximately 90 μW using neutral density filters and measured with a Metrologic silicon radiometer calibrated to a Scientech power meter. The emission signals were observed with either a cooled RCA 31034 photomultiplier tube (PMT) or a Tracor Northern microchannel plate intensified diode array filtered by a Schott RG-695 long pass filter and corrected to 90 μW incident power during data reduction. A long wavelength cutoff of $\sim$850 nm was provided by the falloff in detector response. In the infrared experiments, the monochrometer bandpass was set to 75 nm and the incident power set to about 50 μW, with similar corrections made to the emission signals during data reduction. The infrared excitation light was filtered with a 3-mm-thick silicon window to block radiation below 1.05 μm and the power measured with a calibrated PbS detector by a chopper and lock-in amplifier. In the infrared both steady state and pseudopulsed experiments were performed and are described below. Timing experiments in the UV were done near the peak in the UV absorption feature, using the mixed 351–364 nm lines (intensity ratio of 33:67) from an argon-ion laser, modulated by a fast acousto-optic switch. The rise and fall times of the broadband emission feature at 825 nm was viewed with a cooled RCA 31034 PMT fitted with a Schott RG-695 long pass filter. Pulses from the PMT were sent to a Stanford Research Systems SR400 photon counter and recorded with a Tracor Northern 1505 Signal Averager operated in multichannel scaling mode and coupled to a laboratory computer. In the UV and visible experiments, the excitation light was focused onto the sample with a spot size of approximately three times the glass shell diameter, whereas in the IR the spot size was twice that used in the UV/visible.

The near infrared emission feature at 825 nm only occurs at temperatures below 10 K and increases with decreasing temperature.[9] If the excitation light were simply heating the sample, the emission signal would decrease. There is secondary emission in the 825-nm region due to ball fluorescence from tritium radiation and from the UV and visible excitation sources that is relatively constant over the temperature range of 4.5 to 20 K. Since the DT sample inside the glass ball could not be removed in order to provide a blank reference the following procedure was used to remove the unwanted emission signals at 825 nm. Four experiments were done at each wavelength, one with the excitation source on and one off, at 4.5 and at 12 K, respectively. Using this data, the ratio R of the light-on enhanced 825-nm emission to the light-off emission at 4.5 K, corrected for 90-μW light intensity, is given by

$$R=\frac{(\mathrm{On}_c-\mathrm{Off}_c)\times 90\ \mu\mathrm{W}/I_c-(\mathrm{On}_w-\mathrm{Off}_w)\times 90\ \mu\mathrm{W}/I_w}{(\mathrm{Off}_c-\mathrm{Off}_w)}\ , \tag{1}$$

where the subscripts c and w indicate "cold" and "warm" and I is the actual measured intensity. In the infrared experiments $\mathrm{On}_w=\mathrm{Off}_w$. A value of one was added to the above ratio and represents the no enhancement value.

III. RESULTS AND DISCUSSION

Figure 1 shows the integrated emission intensity from 720 to 850 nm as a function of the wavelength of light incident onto solid D-T at 4.5 K. Also plotted in Fig. 1(a) is the UV absorption data of solid D-T at 5 K from Fearon *et al.*[6] and in Fig. 1(b) is the IR absorption of solid T_2 at 8 K from Richardson *et al.*[4] Based on the IR absorption positions in H_2 and D_2, the IR absorption in solid D-T should be shifted slightly to the red ($\sim$20 nm) from the similar absorption in T_2. The shape of the UV enhancement signal follows closely the published UV absorption spectrum for the $1S$ to continuum bubble transition in solid D-T. The enhancement with IR pumping is not very similar to the expected $1S$ to $1P$ IR absorption in solid D-T, but appears in the general vicinity. The relative absorbance strength of the UV line to the IR line in solid D-T is not known and the absolute frequency and shape of the IR line is also unknown. There is no enhancement in 825-nm emission from excitation in the 440- to 700-nm region. Similarly there is also no absorption from 440 to 950 nm.[4] Figure 1(a) suggests that the 825-nm emission and the UV absorption are related to a common species, that being electrons that are not initially bound to hydrogen atoms or molecules. Figure 1(b) on the other hand, is difficult to interpret.

The time response of the enhancement is different for UV vs IR enhanced emission. For UV pumping at the sample temperature of 4.5 K, the enhanced emission rises

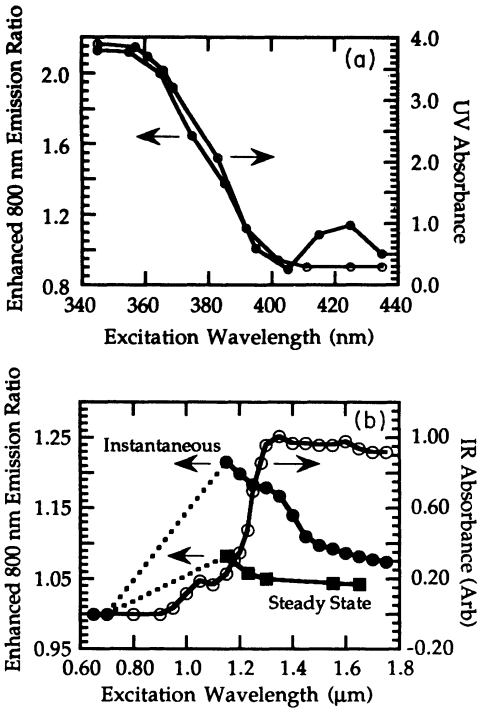

FIG. 1. Integrated emission intensity from 720 to 850 nm as a function of the wavelength of light incident onto solid D-T at 4.5 K. Also plotted in (a) is the UV absorption data of solid D-T at 5 K (Ref. 6) and (b) is the IR absorption data of solid T_2 at 8 K (Ref. 4).

on a time scale of ~ 28 μs and falls with an ~ 18 μs time scale. The UV enhanced signal overshoots the long-time steady-state value by 5–10 % whereas the IR enhanced signal overshoots by 50 to 75 % both having similar settling times of ~ 25 sec. In Fig. 1(b), we plot both the "instantaneous" maximum and long-time steady-state enhanced signal for IR pumping while in Fig. 1(a), we only plot the final steady-state enhanced signal for UV pumping. Correcting Eq. (1) for power and spot size, the maximum instantaneous response for IR pumping (at 1.15 μm) is $\sim 30\%$ greater than the maximum UV value at 345 nm. However, the maximum steady-state value at 1.15 μm is $\sim 50\%$ lower than the UV maximum.

Figure 1(a) also shows an additional feature at about 425 nm not readily observed in the UV absorption spectra. Note, however, that the UV absorbance is small but not zero from 410 to 435 nm but is zero from 440 to 950 nm.[6] While the power dependence of this feature was not studied in detail, it was noted that by increasing the power from 90 to 150 μW, the 825-nm enhancement due to excitation at 425 nm was still visible but the enhancement factor ratio at 425 nm vs 365 nm decreased by a factor of ~ 5.

Having related an emission at 825 nm in irradiated solid hydrogen to electrons, we plot its wavelength versus temperature in solid D-T between 4.5 and 10 K in Fig. 2. Over this temperature range the emission feature shifts to the red about 8 nm. In solid T_2 we find this emission shifts 3 ± 2 nm towards the red as compared to D-T.

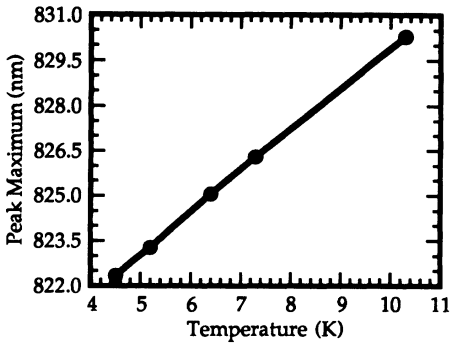

FIG. 2. Emission peak wavelength vs temperature for the emission feature near 825 nm in solid D-T.

We have previously reported the observation of both optical pulses[9] and heat spikes[16] from solid tritiated hydrogen. A heat spike occurs when unpaired atoms recombine en masse releasing energy which heats the sample. At roughly the same time the emission feature at 825 nm "flashes" for milliseconds with an intensity over an order of magnitude larger than the steady-state value.[9] We also find the peak wavelength of the flash is shifted about 40 nm to the red as compared to the steady-state emission before the flash. This shift compared with the wavelength shift versus temperature shown in Fig. 2 implies the sample is much warmer by the time this flash occurs.

These shifts can be compared to the isotope shifts for the IR and UV absorptions. There is an isotope shift of about 400 nm towards the red in the $1S$ to $1P$, IR absorption going from D_2 to H_2 whereas the corresponding isotope shift for the $1S$ to continuum, UV absorption is about 300 nm towards the red.

Finally, we report a triplet structure in the steady-state 825-nm emission in solid T_2, whereas no structure was resolved in the solid D-T mixture. This emission along with the triple Gaussian fit is shown in Fig. 3. This triplet may be similar in nature to the triplet feature found in the IR absorption of proton irradiated D_2 (Ref. 17) and the less well-resolved doublet feature in the IR absorption of H_2 and D_2 containing small amounts of T_2.[5] In proton irradiated D_2 the spacing between the 3 IR absorption

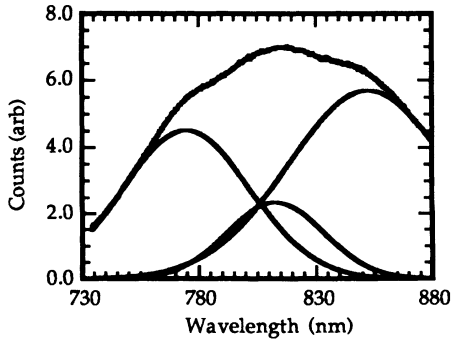

FIG. 3. Emission feature near 825 nm in solid T_2 at 6.4 K together with a three Gaussian fit.

peaks, moving towards higher energy is 0.128 and 0.087 eV, whereas the spacing between the T_2, 825-nm emission peaks is 0.076 and 0.080 eV. The triplet structure is though to be due to either crystal asymmetry of the hcp lattice, or to trapping sites with different equilibrium radii.[17]

To explain many of the above observations we turn to the spherical square-well model, which with previously published parameters[7] (radius= 0.58 nm, depth= 3.8 eV) has 4 bound states, the 1*S*, 1*P*, 1*D*, and 2*S* states 3.0, 2.2, 1.2, and 0.8 eV below the conduction band, respectively. Thus, there are other bound states in the electron bubble than just those involved in the IR and UV absorptions and there should be additional absorption and/or emission signatures not yet observed. The feature at 425 nm may be an example. Excited states increase the width of the potential well, thus agreement between absorption experiments and calculated transitions between states calculated from a static bubble model require the Frank Condon principle.[5] If the 825-nm emission (1.5 eV) is due to an excitation and fluorescent decay of electron bubbles, the transition energies will be relatively close to those calculated from the static model and the 2*S* to 1*P* transition (1.4 eV) has about the right energy. If the 825-nm emission is due to a fluorescent decay during bubble formation, the energy levels need to be recalculated. Using an anharmonic potential, a likely mechanism would involve photon emission resulting from a mobile electron or polaron dropping into a vacancy followed by a nonradiative lattice expansion to form the stable bubble state. The potential energy diagram would show a radiative vertical transition to high on the inner wall at a vacancy radius of ~ 0.36 nm, followed by a relaxation down the wall to the equilibrium bubble radius of 0.58 nm. Calculating the density and/or temperature dependence for the above transition energies and comparing them with the shifts in the UV, IR, and 825-nm features should further elucidate the nature of the emission. Although a similar calculation was done for electron bubbles in liquid hydrogen,[18] no calculation exists for the solid phase.

Although attributing the 825-nm emission to the electron bubble is appealing, we cannot completely exclude electron recombination with a charged species such as H_3^+. The idea of H_3^+ or H_9^+ in the irradiated hydrogen lattice is not a new one. Brooks *et al.* considered D_3^+ as mobile polaron holes and D_9^+ as trapped clusters in modeling their timing data.[3] Stenum *et al.* attribute an emission feature at 275 nm (25 nm width) in electron irradiated solid D_2 to the radiative bound-free transition, $3d\,^2E' \rightarrow 2p\,^2E'$, of the D_3^* molecule after electron recombination of D_3^+.[19,20] The assignment to this D_3^* transition was chosen over the 75 nm wide, $a\,^3\Sigma_g^+ \rightarrow b\,^3\Sigma_u^+$ transition in D_2 also at 275 nm observed in gaseous deuterium, because the linewidth in the solid was too narrow. This 275-nm emission feature was ~ 100 times weaker than the 825-nm emission and no temperature dependence was reported. Fearon and Souers also observed an emission line at 275 nm (50 nm width) in solid D-T which persisted upon warming the sample to the liquid state.[21] Thus if the assignment of the 275-nm emission to D_3^* is correct, the intensity and temperature dependence at least suggest that D_3^* is not involved in the 825-nm emission but does not necessarily exclude D_3^+ or D_9^+.[22,23]

IV. SUMMARY

We have observed that pumping the UV, 1*S* to continuum transition, which photoejects an electron from a bubble, gives rise to enhanced emission at 825 nm. This observation implies the emission at 825 nm is due to unbound electrons in solid irradiated hydrogen. Pumping the IR transition does not necessarily detrap the electron making interpretation of the response at 825 nm unclear. We have also observed that the steady-state emission shifts ~ 8 nm towards the red upon increasing the temperature from 4.5 to 10 K. Finally, the same emission in pure solid T_2, is shifted ~ 3 nm towards longer wavelengths and contains a triplet structure similar to the triplet structure observed in absorption measurements of the 1*S* to 1*P* transition of electron bubbles. These wavelength shifts and the triplet structure imply the emission at 825 nm is related to electron bubbles, but more modeling of electron bubble dynamics is necessary before a more specific assignment can be made.

ACKNOWLEDGMENTS

We would like to thank Tom Bernat, John Lindl, and Mike Campbell for their support of this work. We gratefully acknowledge the financial support of the Air Force High Energy Density Materials Program at the Phillips Laboratory and the NASA Lewis Research Center. This work was performed under the auspices of the U.S. Department of Energy by the Lawrence Livermore National Laboratory under Contract No. W-7405-ENG-48.

[1] P. C. Souers, E. M. Fearon, R. L. Stark, R. T. Tsugawa, J. D. Poll, and J. L. Hunt, Can. J. Phys. **59**, 1408 (1981).
[2] S. K. Bose and J. D. Poll, Can. J. Phys. **63**, 67 (1987).
[3] R. L. Brooks, S. K. Bose, J. L. Hunt, Jack R. MacDonald, J. D. Poll, and J. C. Waddington, Phys. Rev. B **32**, 2478 (1985).
[4] J. H. Richardson, S. B. Deutscher, P. C. Souers, R. T. Tsugawa, and E. M. Fearon, Chem. Phys. Lett. **81**, 26 (1981).
[5] J. D. Poll, J. L. Hunt, P. C. Souers, E. M. Fearon, R. T. Tsugawa, J. H. Richardson, and G. H. Smith, Phys. Rev. A **28**, 3147 (1983).
[6] E. M. Fearon, R. T. Tsugawa, P. C. Souers, J. D. Poll, and J. L. Hunt, Fusion Tech. **8**, 2239 (1985).
[7] J. A. Forrest, J. L. Hunt, and R. L. Brooks, Can. J. Phys. **68**, 1247 (1990).
[8] A. Gedanken, B. Raz, and J. Jortner, Chem. Phys. Lett. **14**, 326 (1972).
[9] E. R. Mapoles, F. Magnotta, G. W. Collins, and P. C. Souers, Phys. Rev. B **41**, 11 653 (1991).
[10] F. Weinhaus, H. Meyer, S. M. Myers, and A. B. Harris, Phys. Rev. B **7**, 2960 (1973); M. Bloom, Physica **23**, 767 (1957).

[11]R. Leach, Ph.D. thesis, University of Wisconsin, 1972 (unpublished), available from University Microfilms, Ann Arbor, MI.

[12]A. S. Iskovskikh, A. Ya. Katunin, I. I. Lukashevich, V. V. Sklyarevskii, V. V. Suraev, V. V. Filippov, M. I. Filippov, V. A. Shevtsov, Zh. Eksp. Teor. Fiz. **91**, 1832 (1986) [Sov. Phys. JETP **64**, 1085 (1986)].

[13]A. A. Levchenko, L. P. Mezhov-Deglin, and I. E. Shtinov, Pis'ma Zh. Eksp. Teor. Fiz. **54**, 238 (1991) [JETP Lett. **54**, 234 (1991)]. Note the diffusion of electrons measured in this paper follow the temperature dependence of Ebner and Sung's model to well below half of the triple point temperature, where NMR measurements of molecular motion are difficult.

[14]C. Ebner and C. C. Sung, Phys. Rev. A **5**, 2625 (1971).

[15]J. A. Forrest, R. L. Brooks J. L. Hunt, B. Stenum, J. Schou, H. Sorensen, P. Gurtler, F. Magnotta, E. R. Mapoles, P. C. Souers, and G. W. Collins, Phys. Rev. B **46**, 13 820 (1992).

[16]G. W. Collins, E. M. Fearon, J. L. Maienschein, E. R. Mapoles, R. T. Tsugawa, P. C. Souers, and J. R. Gaines, Phys. Rev. Lett. **65**, 444 (1990).

[17]M. A. Selen, R. L. Brooks, J. L. Hunt, J. D. Poll, J. R. MacDonald, and J. C. Waddington, Nucl. Instrum. Methods B **2**, 720 (1984).

[18]Toru Miyakawa and D. L. Dexter, Phys. Rev. **184**, 166 (1969).

[19]B. Stenum, J. Schou, H. Sorensen, and P. Gurtler, J. Chem. Phys. **98**, 126 (1993).

[20]A. B. Raksit, R. F. Porter, W. P. Garver, and J. J. Leventhal, Phys. Rev. Lett. **55**, 378 (1985).

[21]E. M. Fearon and P. C. Souers (private communication).

[22]We note that the difference in energy between the H_3^+ and $3d^2E'$ in H_3^* is 1.5 eV or $\sim$825 nm. Mitchel (Ref. 23) has shown that electron recombination with H_3^+ yields a H_3^* about 8% of the time, requiring radiative stabilization; this state is subsequently predissociated.

[23]J. B. A. Mitchel, Phys. Rep. **186**, 215 (1990).